ISSN: 0067-2904

Impact of ZnO Atomic Ratio on Structural, Morphological and Some Optical Properties of $(SnO_2)_{1-x}$ $(ZnO)_x$ Thin Films

Donia Yas Khudair[*1], Ramiz Ahmed Al Ansari[1], Mervat K.Tameem[1], Ghuson H.Mohammed[2], Kadhim A.Aadim[2]

[1]Department of Physics, College of Science for Women, Baghdad University, Baghdad, Iraq
[2]Department of Physics, College of Science, University of Baghdad

Received: 13/5/ 2019 Accepted: 28/ 8/2019

Abstract

In this work, SnO_2 and $(SnO_2)_{1-x}(ZnO)_x$ composite thin films with different ZnO atomic ratios (x=0, 5, 10, 15 and 20%) were prepared by pulsed laser deposition technique on clean glass substrates at room temperature without any treatment. The deposited thin films were characterized by x-ray diffraction atomic force microscope and UV-visible spectrophotometer to study the effect of the ZnO atomic ratio on their structural, morphological and optical properties. It was found that the crystallinety and the crystalline size vary according to ZnO atomic ratio. The surface appeared as longitudinal structures which was convert to spherical shapes with increasing ZnO atomic ratio. The optical transmission and energy gap increased with increasing ZnO atomic ratio.

Keywords: ZnO, composite, structural properties, morphological properties, optical properties

تأثير النسبة الذرية ZnO على الخواص التركيبية والمورفولوجية والبصرية للأغشية الرقيقة $(SnO_2)_{1-x}(ZnO)_x$

دنيا ياس خضير[*1]، رامز احمد الانصاري[1]، ميرفت كاظم تميم[1]، غصون حميد محمد[2]، كاظم عبد الواحد عادم[2]

[1]قسم الفيزياء، كليه العلوم للبنات، جامعة بغداد، بغداد، العراق
[2]قسم الفيزياء، كلية العلوم، جامعة بغداد، بغداد، العراق

الخلاصة

تم في هذا العمل تحضير الأغشية الرقيقة SnO_2 و الأغشية الرقيقة لمزيج $(SnO_2)_{1-x}(ZnO)_x$ و بنسب ذرية مختلفة من ZnO (x=0, 5, 10, 15 and 20%) بواسطة تقنية ترسب الليزر النبضي على ركائز زجاجية في درجة حرارة الغرفة. تم تشخيص الأفلام الرقيقة المحضرة بواسطة حيود الأشعة السينية و مجهر القوة الذرية و طيف الامتصاص المرئية – فوق البنفسجية لدراسة تأثير نسبة ZnO على الخصائص التركيبية والمورفولوجية والبصرية للأفلام المحضرة. وقد وجد أن درجة التبلور والحجم البلوري تختلف وفقا لنسبة ZnO. تحولت طوبوغرافية السطح من أشكال طولية إلى أشكال كروية مع زيادة نسبة ZnO. ازدادت فجوة الطاقة البصرية مع زيادة نسبة ZnO.

Introduction

Tin oxide (SnO_2) is an n-type semiconductor which has a direct band gap of 3.5-3.6 eV [1]. SnO_2 thin film is one of the important transparent conducting oxides applied in various manufacturing fields [2] such as transparent electrodes in flat-panel displays, light-emitting diodes and solar cell applications [3]. Also, SnO_2 is employed in a wide range of gas sensing methods [4]. SnO_2 thin films are prepared by different techniques such as radio frequency sputtering technique [6], chemical solution deposition [7], sol- gel immersion method [8] and pulsed laser deposition [9].

*Email:dunia9285 @gmail.com

Tin oxide is doped with many elements, such as SnO_2: Sb [10] and Fe-doped SnO_2 [7], in order to control its structural, optical and electrical properties or to obtain nanostructures useful in many applications [11]. Also, SnO_2 was developed with many materials as a composite, including graphene:SnO_2 [12] and ZnO:SnO_2 composite thin film annealed at 873 K [13]. In this work, ZnO:SnO_2 was deposited by a pulsed laser deposition technique at different atomic ratios without any treatment to study the effect of ZnO atomic ratio on thin film properties.

Experimental Part

Tin oxide powder (SnO_2) of 99.9 % purity and zinc oxide powder (ZnO) of 99.9 %purity, obtained from FERAK company, were mixed as $(SnO_2)_{1-x}(ZnO)_x$, where x= 0, 5, 10, 15 and 20% atom ratio. The $(SnO_2)_{1-x}(ZnO)_x$ powders with different x atomic ratios were pressed as targets with 1cm diameter under 3 ton press. $(SnO_2)_{1-x}(ZnO)_x$ thin films were prepared by pulsed laser deposition technique (PLD) under 10^{-2} mbar vacuum at room temperature. Q-switched pulsed laser (DIAMOND-288, λ = 1064 nm) was used. The laser power supply tuned at 900 mJ peak power. The laser beam was focused onto the target throw the glass chamber. The laser beam was incident with 45° onto the target. The substrate was placed parallel to the target surface at 2 cm separation distance. The prepared samples were examined by x-ray diffraction (XRD), atomic force microscope (AFM) and UV-visible absorbance spectroscopy to find the basic properties for the prepared thin films without any treatment.

Results and discussion

Figure-1 shows the x-ray diffraction patterns of the pure SnO_2 thin film and of that mixed with ZnO at different atomic ratios. X-ray diffraction curves showed that all samples had a polycrystalline structure, with many peaks appearing at 26.52°, 33.81°, 37.92°, 51.73°, 54.75°, 61.84°, 64.69°, 66.00°, 71.25° and 78.72° for the pure sample, corresponding to (110), (101), (200), (211), (220), (310), (112), (301), (202) and (321) planes for the tetragonal SnO_2, that matches the values in the standard card number 96-500-0225. There are slight differences in the diffraction angles with varying zinc oxide ratios due to stresses within the lattice [14]. The crystallization was enhanced with increasing ZnO ratio to 10%, where the additive acted as a catalyst for crystalline growth [15]. The higher rate of ZnO atomic ratio reduced the crystallization rate. New peaks appeared at 31.73° and 36.21° which were attributed to the crystalline planes (100) and (101) for ZnO at 15% and 20% and matched with the standard card No. 96-901-1663. The full width of the peaks changed in response to the changes in the strain applied on lattice, due to the particle size change as shown by Sherrer's equation [16].

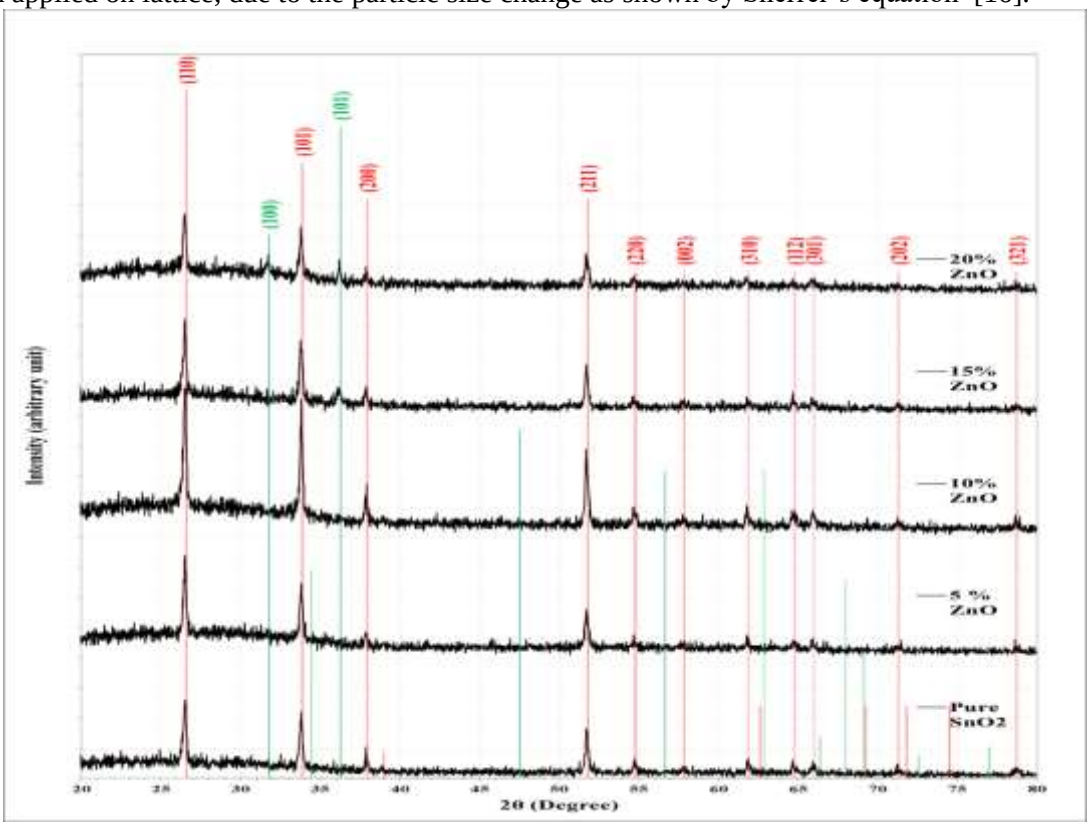

Figure 1-X-ray diffraction curves of pure SnO_2 and that mixed with different ZnO atomic ratio.

Table-1 shows the values of Bragg's diffraction angles (2θ), the full width of half maximum (FWHM), inter-planer distance (d_{hkl}), the crystallite size (C.S), and the corresponding Miller indices of the standard cards (hkl).

Table 1-Comparison between calculated and standard d_{hkl}, 2Θ, the C.S and phase for $(SnO_2)_{1-x}(ZnO)_x$ thin films at different x atomic ratios.

Sample	2θ (Deg.)	FWHM (Deg.)	d_{hkl} Exp.(Å)	d_{hkl} Std.(Å)	C.S (nm)	Av. C.S (nm)	Phase	hkl	Card No.
Pure SnO_2	26.5248	0.3309	3.3577	3.3496	24.7	26.7	Tet.SnO_2	(110)	96-500-0225
	33.8061	0.2837	2.6493	2.6431	29.3		Tet.SnO_2	(101)	96-500-0225
	37.9196	0.2837	2.3708	2.3685	29.6		Tet.SnO_2	(200)	96-500-0225
	51.7258	0.3310	1.7659	1.7639	26.7		Tet.SnO_2	(211)	96-500-0225
	54.7518	0.2836	1.6752	1.6748	31.5		Tet.SnO_2	(220)	96-500-0225
	61.8440	0.3782	1.4990	1.4980	24.5		Tet.SnO_2	(310)	96-500-0225
	64.6809	0.3310	1.4400	1.4382	28.4		Tet.SnO_2	(112)	96-500-0225
	66.0047	0.3783	1.4142	1.4147	25.0		Tet.SnO_2	(301)	96-500-0225
	71.2530	0.4256	1.3224	1.3216	23.0		Tet.SnO_2	(202)	96-500-0225
	78.7234	0.4255	1.2146	1.2145	24.1		Tet.SnO_2	(321)	96-500-0225
With 5% ZnO atomic ratio	26.5248	0.3309	3.3577	3.3496	24.7	30.4	Tet.SnO_2	(110)	96-500-0225
	33.8534	0.2837	2.6457	2.6431	29.3		Tet.SnO_2	(101)	96-500-0225
	37.9196	0.2191	2.3708	2.3685	38.3		Tet.SnO_2	(200)	96-500-0225
	51.7258	0.3310	1.7659	1.7639	26.7		Tet.SnO_2	(211)	96-500-0225
	54.6572	0.2292	1.6779	1.6748	39.0		Tet.SnO_2	(220)	96-500-0225
	61.7967	0.2363	1.5000	1.4980	39.2		Tet.SnO_2	(310)	96-500-0225
	64.7281	0.2837	1.4390	1.4382	33.2		Tet.SnO_2	(112)	96-500-0225
	65.9102	0.3310	1.4160	1.4147	28.6		Tet.SnO_2	(301)	96-500-0225
	71.3002	0.3310	1.3216	1.3216	29.5		Tet.SnO_2	(202)	96-500-0225
	78.6288	0.6620	1.2158	1.2145	15.5		Tet.SnO_2	(321)	96-500-0225
With 10% ZnO atomic ratio	26.5721	0.2364	3.3519	3.3496	34.5	32.4	Tet.SnO_2	(110)	96-500-0225
	33.8534	0.2364	2.6457	2.6431	35.1		Tet.SnO_2	(101)	96-500-0225
	37.9196	0.2837	2.3708	2.3685	29.6		Tet.SnO_2	(200)	96-500-0225
	51.6785	0.2364	1.7674	1.7639	37.3		Tet.SnO_2	(211)	96-500-0225
	54.7045	0.2363	1.6765	1.6748	37.9		Tet.SnO_2	(220)	96-500-0225
	61.7967	0.2309	1.5000	1.4980	40.1		Tet.SnO_2	(310)	96-500-0225
	64.6336	0.3256	1.4409	1.4382	28.9		Tet.SnO_2	(112)	96-500-0225
	65.9574	0.2836	1.4151	1.4147	33.4		Tet.SnO_2	(301)	96-500-0225
	71.3002	0.4256	1.3216	1.3216	23.0		Tet.SnO_2	(202)	96-500-0225
	78.6761	0.4255	1.2152	1.2145	24.1		Tet.SnO_2	(321)	96-500-0225
With 15% ZnO atomic ratio	26.6194	0.2837	3.3460	3.3496	28.8	27.8	Tet.SnO_2	(110)	96-500-0225
	33.7589	0.2364	2.6529	2.6431	35.1		Tet.SnO_2	(101)	96-500-0225
	36.1702	0.2836	2.4814	2.4754	29.5		Hex. ZnO	(101)	96-901-1663
	37.8723	0.2837	2.3737	2.3685	29.6		Tet.SnO_2	(200)	96-500-0225
	51.7258	0.3310	1.7659	1.7639	26.7		Tet.SnO_2	(211)	96-500-0225
	54.7045	0.5200	1.6765	1.6748	17.2		Tet.SnO_2	(220)	96-500-0225
With 20% ZnO atomic ratio	26.5248	0.2364	3.3577	3.3496	34.5	27.4	Tet.SnO_2	(110)	96-500-0225
	31.7258	0.4255	2.8181	2.8137	19.4		Hex. ZnO	(100)	96-901-1663
	33.8061	0.3310	2.6493	2.6431	25.1		Tet.SnO_2	(101)	96-500-0225
	36.2175	0.2836	2.4783	2.4754	29.5		Hex. ZnO	(101)	96-901-1663
	37.8723	0.3310	2.3737	2.3685	25.4		Tet.SnO_2	(200)	96-500-0225
	51.7258	0.3310	1.7659	1.7639	26.7		Tet.SnO_2	(211)	96-500-0225
	54.7518	0.2836	1.6752	1.6748	31.5		Tet.SnO_2	(220)	96-500-0225

Figure-2 shows the change in the average crystallite size (C.S) (calculated from the average of calculated values in Table-1) with the change in ZnO ratio. When ZnO ratio increased from 0 to 10%, the average C.S was increased from 26.7 to 32.4 nm, while it was decreased with more increasing the ZnO percentage to 27.4 nm at 20% due to the variation of the nanostructure form.

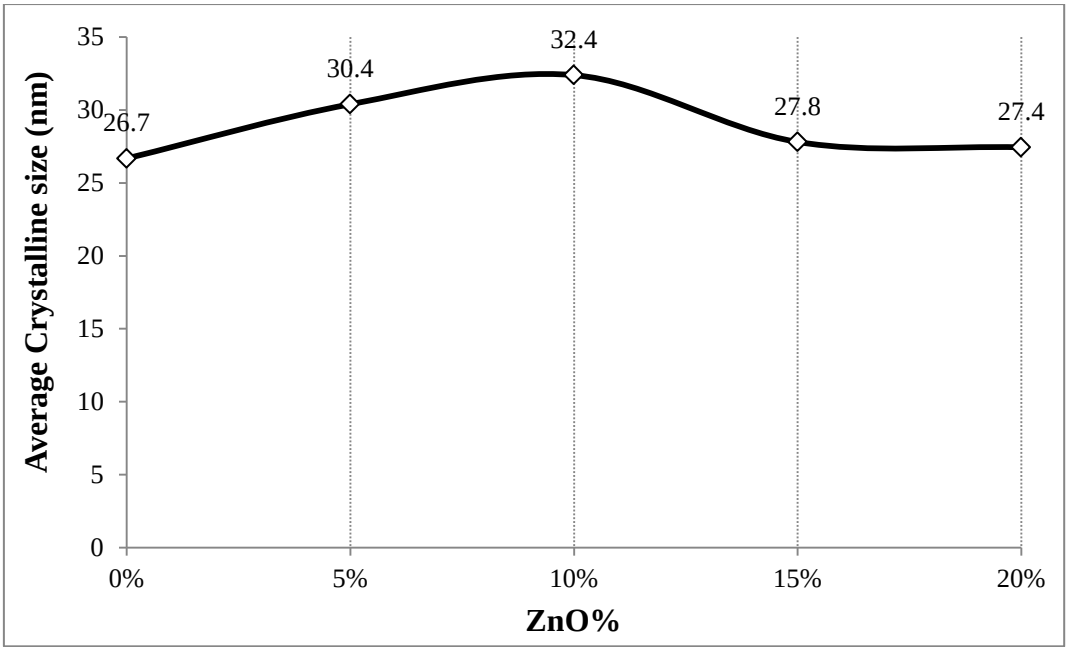

Figure 2-Average crystallite size versus ZnO atomic ratio for $(SnO_2)_{1-x}(ZnO)_x$ thin films.

Figure-3 shows the variation of lattice constants (a and c) for the tetragonal SnO_2 with changing the ZnO mix ratio. The lattice constant (a) was reduced to a minimum value of 4.732 Å with increasing ZnO atomic ratio to 15% in the prepared thin films, and then increased by increasing ZnO content up to 20%. On the other hand, it was observed that the lattice constant (c) has an apposite behavior. The results were consistent with the improvement of the grain size and shape of the nanostructures shown by the AFM. The extension of (c) unit cell and the reduction along (a) orientation were due to Zn ion insertion into the SnO_2 lattice. These result agree with those of a previous sttudy [17].

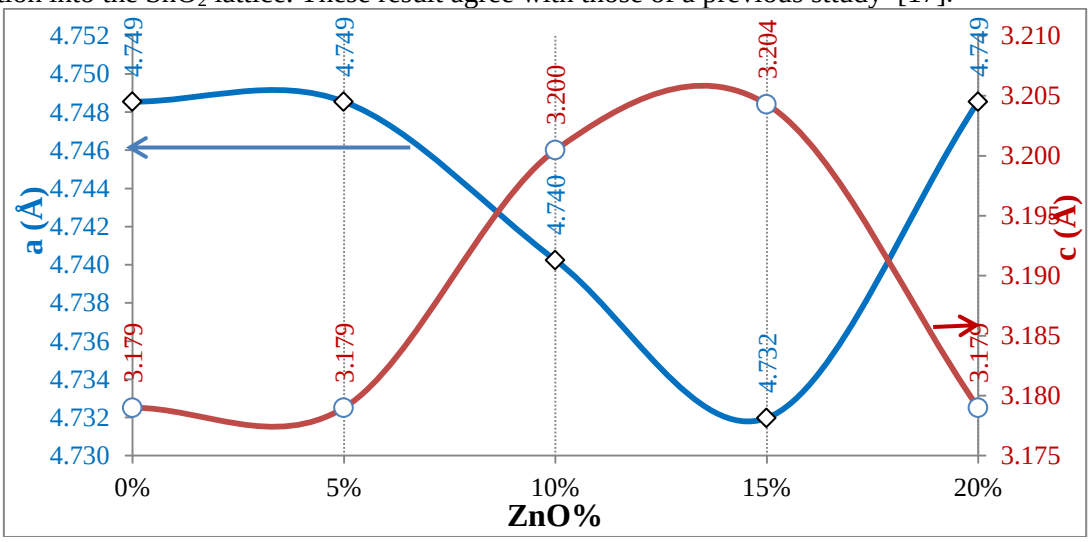

Figure 3-Variation of lattice constants (a and c) for tetragonal SnO_2 with ZnO ratio in $(SnO2)_{1-x}$ $(ZnO)_X$ thin films.

AFM analysis was used to study the surface morphology of $(SnO_2)_{1-x}$ $(ZnO)_X$ thin films at different atomic ratios as shown in Figure- 4, which in turn affected their characteristics. The figure illustrates that the SnO_2 has longitudinal structures with a diameter of 110 nm and a length of 700 nm (measured by ImageJ software). The surface structures have nonhomogeneous distribution. The increase in ZnO atomic ratio to 10% led to an increase of the average grain size from 80.51 to 94.81 nm, while more increasing the ZnO ratio led to a decrease in the average grain size to 65.86 nm at 20% (as shown in

Table-2), converting it into a spherical shape with a homogeneous distribution. It also shows that the average roughness and the root mean square roughness were increased at 5% ZnO and started to decrease at higher ZnO atomic ratios due to variations of nanostructure features [18].

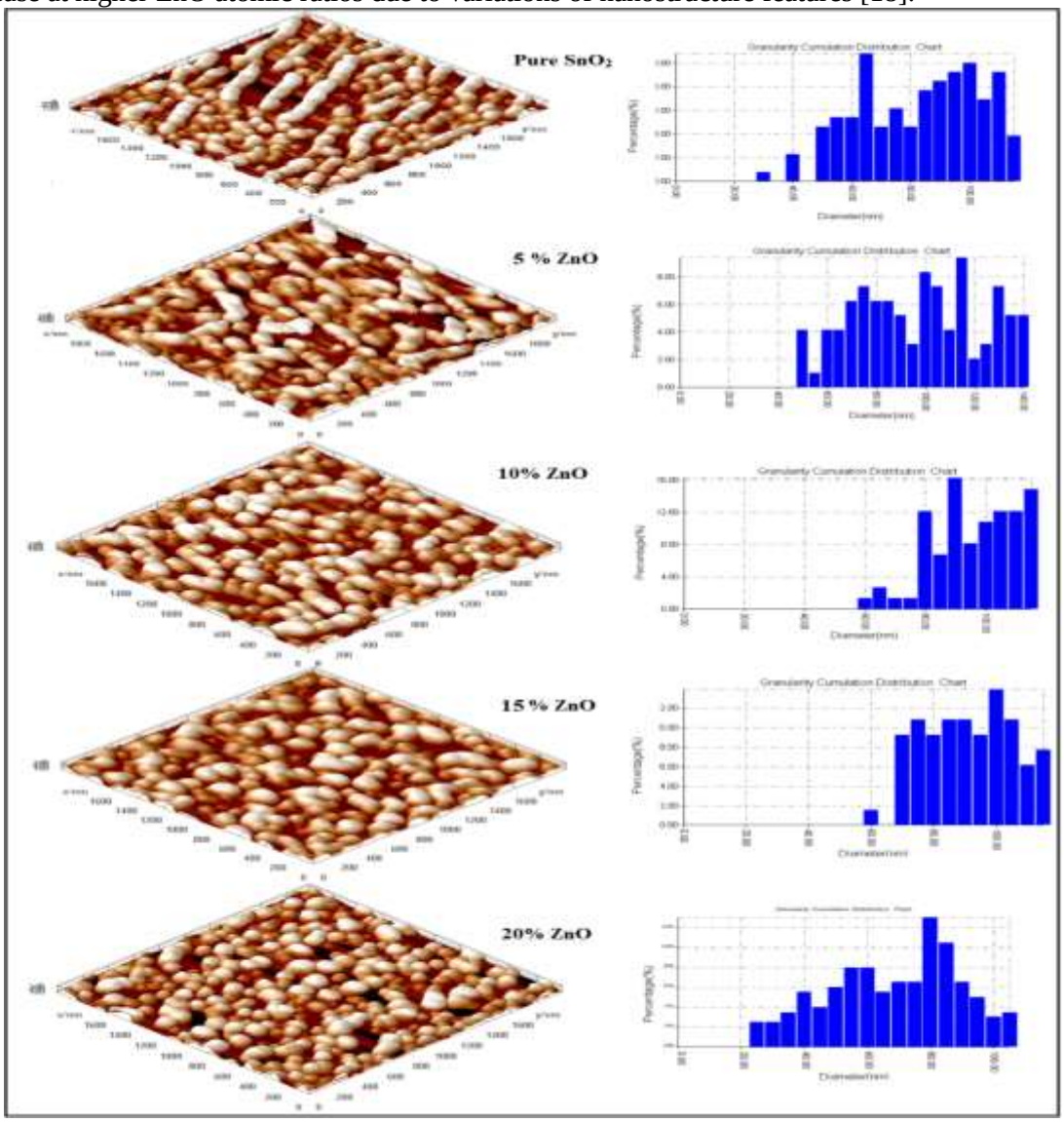

Figure 4-3D AFM images for $(SnO)_{1-x}(ZnO)_x$ thin films and the granular size distribution at different ZnO/SnO_2 atomic ratios.

Table 2-Average grain size, average roughness and root mean square values of $(SnO_2)_{1-x}(ZnO)_x$ at different ZnO/SnO_2 atomic ratios.

Sample	Average grain size (nm)	Average roughness (nm)	Root mean square (nm)
Pure SnO_2	80.51	0.353	0.405
With 5% ZnO	93.73	1.41	1.64
With 10% ZnO	94.81	0.777	0.904
With 15% ZnO	88.57	0.553	0.645
With 20% ZnO	65.86	0.355	0.414

Figure-5 shows the transmittance spectra for $(SnO_2)_{1-x}(ZnO)_x$ thin films, through which the effects of the ZnO/SnO_2 atomic ratios on their optical properties were studied. It can be observed that the optical transmittance is high at long wavelengths (greater than 600 nm) while having low values at

short wavelengths (less than 400 nm). It is also observed that the transmittance increases by increasing the ratio of ZnO due to the change in the crystallization rate or because of the change in the value of the energy gap [19].

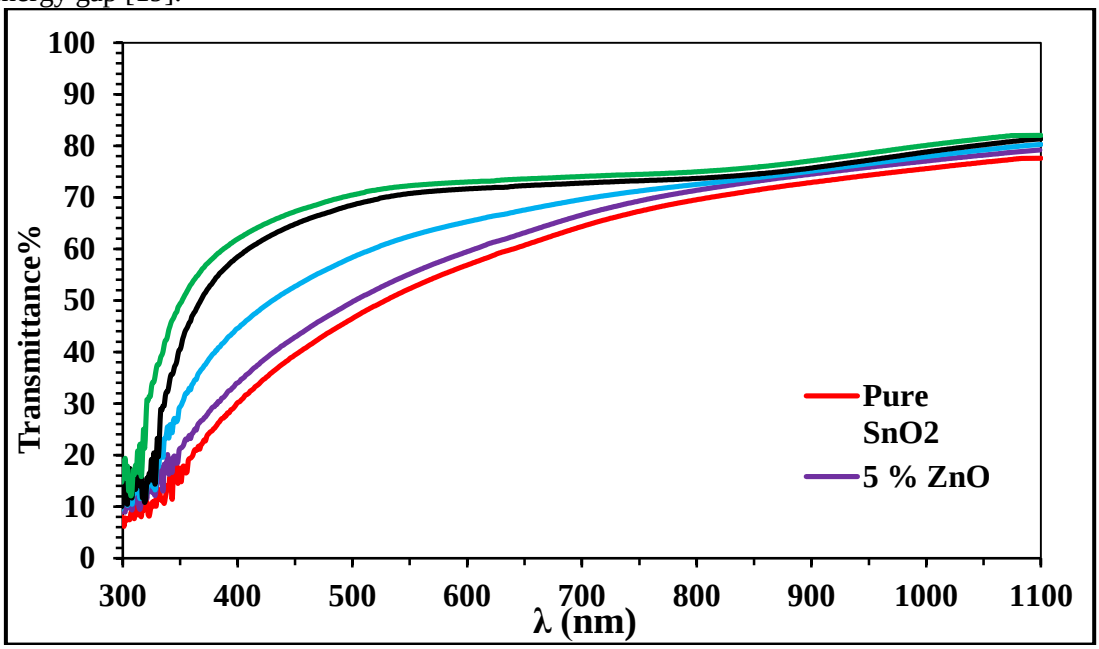

Figure 5-Transmittance spectrum for $(SnO)_{1-x}(ZnO)_x$ thin films at different ZnO atomic ratios.

The direct optical energy gap of the samples was calculated using the Tauc formula [20], where the optical energy gap was calculated from the graphing relationship between $(\alpha h\upsilon)^2$ on the y-axis as a function of the photon energy ($h\upsilon$). Determining the energy gap from the tangent intersect point of the linear region with the x-axis is shown in Figure- 6 for different ZnO/SnO_2 atomic ratios.

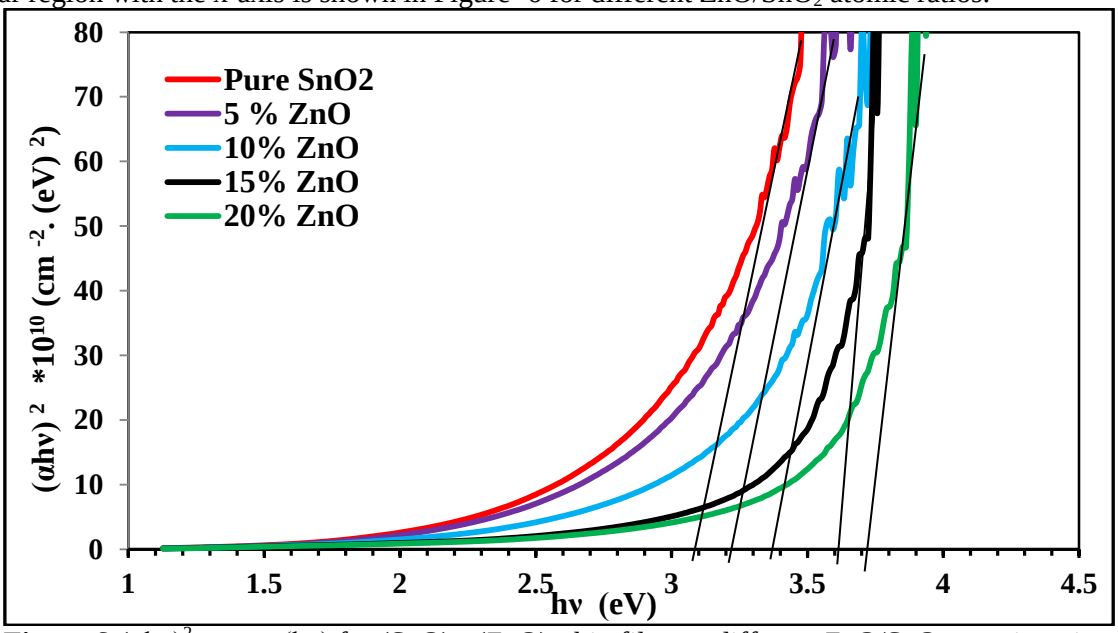

Figure 6-$(\alpha h\upsilon)^2$ versus ($h\upsilon$) for $(SnO)_{1-x}(ZnO)_x$ thin films at different ZnO/SnO_2 atomic ratios.

Figure-7 shows the changes in the values of the direct optical energy gap with the changes in the ZnO/SnO_2 atomic ratios. The figure shows that increasing the ZnO/SnO_2 atomic ratios has increased its values. There are several factors that affect the value of the optical energy gap, such as the difference in distance between the atoms due to lattice strain [21]. The difference in the values of the energy gap from the standard values is due to preparation conditions and the degree of crystallization of the prepared samples. The samples were prepared at room temperature without any treatment and,

hence, the samples had low crystallinity as illustrates in XRD results. The low values of the band gap may be due to the existence of tail states within the band gap [22].

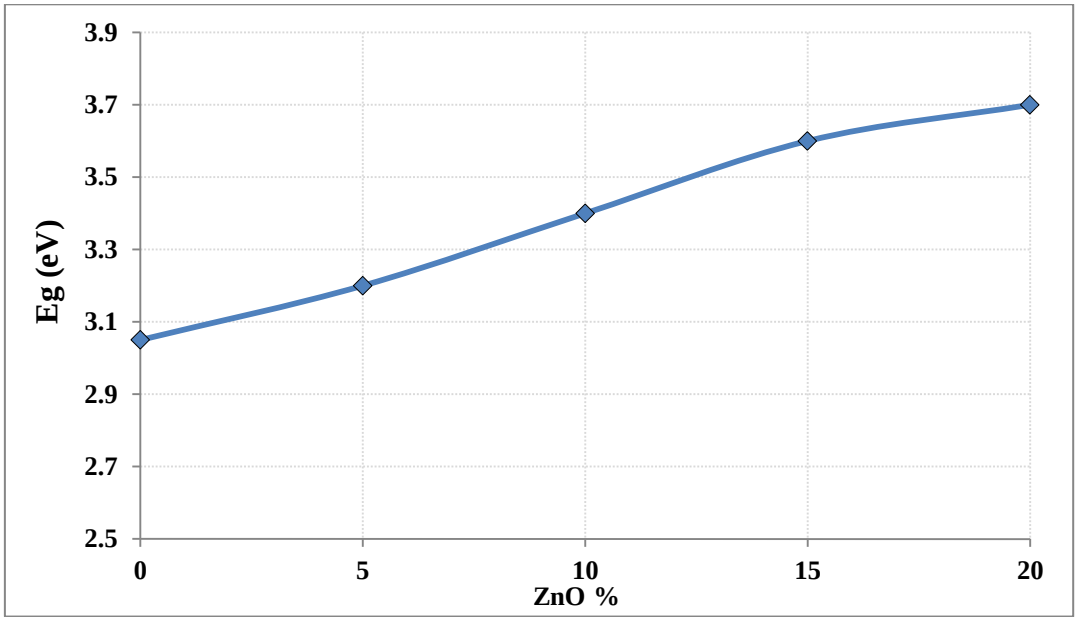

Figure 7-Variations of the optical energy gap for $(SnO)_{1-x}(ZnO)_x$ thin films with ZnO/SnO_2 atomic ratios.

Conclusions

The results of the examination of the $(SnO)_{1-x}(ZnO)_x$ thin films prepared on glass substrates at room temperature using PLD technique, without any treatment, illustrate polycrystalline structures for the prepared samples. The sample with 10% ZnO atomic ratio has the maximum crystallite size.

AFM images illustrated longitudinal structures with a diameter of 110 nm and a length of 700 nm for pure samples. The increase in ZnO ratio to 5% led to an increase in the average grain size, which was decreased with higher ZnO atomic ratios. The particles were converted into spherical shapes with a homogeneous size distribution.

The UV-visible absorption measurement for $(SnO)_{1-x}(ZnO)_x$ thin films demonstrated that increasing ZnO ratio leads to increased transparency and energy gap but with values less than the standard value for bulk samples.

References

1. N. Sin, S. Ahmad, M. Malek, M. Mamat, and Rusop, M. **2013**. Improvement sensitivity humidity sensor based on ZnO/SnO_2 cubic structure, *IOP Conf. Ser. Mater. Sci. Eng.*, **46**:1–7.
2. Fahad, O.A., Al-Jumaili, H.S. and Suhail, M.H. **2014**. Studies on spray pyrolised nanostructured SnO_2 thin films for H_2 gas sensing application, *Adv. Environ. Biol.*, **17**(2):125–141.
3. Klein, A. **2010**. Transparent Conducting Oxides for Photovoltaics: Manipulation of Fermi Level, Work Function and Energy Band Alignment, *Materials (Basel)*, **3**(11): 4892–4914.
4. Jianwei G., Chena, Q. and Feib, W. **2004**. Micromachined nanocrystalline SnO_2 chemical gas sensors for electronic nose, *Sensors Actuators B Chem.*, (102): 117–125.
5. Bagheri-Mohagheghi, M.M., Shahtahmasebi, N., Alinejad, M.R., Youssefi, A. and Shokooh-Saremi, M. **2009**. Fe-doped SnO_2 transparent semi-conducting thin films deposited by spray pyrolysis technique: Thermoelectric and p-type conductivity properties, *Solid State Sci.*, **11**(1): 233–239.
6. Baco, S., Chik, A. and Yassin, F.M. **2012**. Study on Optical Properties of Tin Oxide Thin Film at Different Annealing Temperature, *J. Sci. Technol.*, **4**: 61–72.
7. Trivedi, S.J. and Joshi, U.S. **2017**. Resistive switching properties of highly transparent SnO_2: Fe, *J. Nano- Electron. Phys.*, 9(1), pp:2–6.
8. Coutts, T. and Mason, T. **1999**. Transparent Conducting Oxides : Status and Opportunities in Basic, *195th Meet. Electrochem. Soc.*, August, pp:1–15.

9. Preiß, E.M., Rogge, T., Krauß, A. and Seidel, H. **2015**. 'Gas sensing by SnO_2 thin films prepared by large-area pulsed laser deposition', *Procedia Eng.*, **120**: 88–91.

10. Babar, A.R., Shinde, S.S., Moholkar, A.V., Bhosale, C.H., Kim, J.H. and Rajpure, K.Y. **2011**. 'Physical properties of sprayed antimony doped tin oxide thin films: The role of thickness', *J. Semicond.*, **32**(5): 053001–8.

11. Kim, S.S., Na, H.G., Kim, H.W., Kulish, V. and Wu, P. **2015**. 'Promotion of acceptor formation in SnO_2 nanowires by e-beam bombardment and impacts to sensor application', *Sci. Rep.*, **5**: 1–12.

12. Seema, H., Christian Kemp, K., Chandra, V. and Kim, K.S. **2012**. 'Graphene-SnO_2 composites for highly efficient photocatalytic degradation of methylene blue under sunlight', *Nanotechnology*, **23**(35): 1–8.

13. Sinha, S.K. **2016**. 'Tunable structural, optical and electrical properties of annealed ZnO-SnO_2 composite thin films deposited by pulsed laser deposition', *Adv. Mater. Lett.*, **7**(4): 319–324.

14. Moridi, A., Ruan, H., Zhang, L.C. and Liu, M. **2013**. 'Residual stresses in thin film systems: Effects of lattice mismatch, thermal mismatch and interface dislocations', *Int. J. Solids Struct.*, **50**(22): 3562–3569.

15. Singh, S., Thiyagarajan, P., K. Kant, P.K. **2007**. Structure , microstructure and physical properties of ZnO based materials in various forms : bulk , thin film and nano, *J. Phys. D Appl. Phys.*, **40**: 6312–6327.

16. P. Scherrer. **1918**. Göttinger Nachrichten Gesell, *Univ. zu Göttingen*, **2**: 98.

17. N. Sin, S. Ahmad, M. Malek, M. Mamat, and M. Rusop. **2013**, Improvement sensitivity humidity sensor based on ZnO/SnO2 cubic structure, *IOP Conf. Ser. Mater. Sci. Eng.*, **46**: 1–7.

18. S.Singh, **2014**. zinc oxide nanostructures; synthesis, characterizations and device applications, *J. Nanoeng. Nanomanufacturing*, **3**: 1–28.

19. A. Bedia, F. Z. Bedia, M. Aillerie, N. Maloufi, and B. Benyoucef. **2015**, Morphological and optical properties of ZnO thin films prepared by spray pyrolysis on glass substrates at various temperatures for integration in solar cell , *Energy Procedia*, **74**: 529–538.

20. H. Fritzche, **1974**, *Amorphous and Liquid Semiconductors*, Plenums pr. New York and London,.

21. M. A. Basyooni, M. Shaban, and A. M. El Sayed. **2017**, enhanced gas sensing properties of spin-coated na-doped zno nanostructured films, *Nat. Publ. Gr.*, **7**: 1–12.

22. V. P. Kunets, N. R. Kulish, V. P. Kunets, and M. P. Lisitsa. **2002**. 'Urbachs rule peculiarities in structures with CdS_xSe_{1-x} nanocrystals', *Semicond. Physics, Quantum Electron. Optoelectron.*, **5**(2): 9–15.